ICES Annual Science Conference 2002

CM 2002/P:10
Shelf Seas Processes:
The Foundation for Ecosystem Understanding

The front on the Faroe Shelf

Karin Margretha H. Larsen, Bogi Hansen, Harald Svendsen and Knud Simonsen

ABSTRACT

The water mass on the Faroe Shelf is distinct from the off-shelf water surrounding the shelf. This difference of water masses is reflected in the temperature and salinity distributions. The on-shelf water is colder and fresher than the off-shelf water throughout most of the year. A temperature/salinity front thus forms, where the on-shelf water meets the off-shelf water. The waters inside the front have a different cycle of primary production and support a different ecosystem from the off-shelf waters and they are important nursery areas for larvae of many commercially important fish stocks. Sea surface temperature measurements from the R/V Magnus Heinason in the period February 1999 to November 2000 show the existence of the front throughout the year except for a short period in autumn, and the largest cross-front gradients are found in the spring. Also, the measurements are used to find typical values for the frontal location and width in various directions across the shelf. The observed characteristics of the front are discussed in relation to bottom topography and proximity to a shelf edge, to the heating/cooling cycle driven by the air-sea heat flux, and to various theories for fronts generated by tidal or wind mixing.

Karin Margretha H. Larsen and Bogi Hansen: Faroese Fisheries Laboratory, P.O.Box 3051, FO-110 Torshavn, Faroe Islands, email: karinl@frs.fo, bogihan@frs.fo. Harald Svendsen: Geophysical Institute, Allegaten 70, N-5007 Bergen, Norway, email: harald.svendsen@gfi.uib.no. Knud Simonsen: University of the Faroe Islands, P. O. Box 2109, FO-165 Argir, Faroe Islands, email: knuds@setur.fo

INTRODUCTION

The Faroe Islands are situated at 62°N 7°W and are surrounded by a shelf, which is approximately described by its 150 m bottom contour. The 200 m bottom contour occupies about 21000 km^2, and the width of the shelf is greatly varying around the islands (Fig. 1). It is only about 12 km wide east of the southernmost island and approximately 50 km wide in the northwest direction. In some areas the topography is smooth with a well-defined shelf break, and in others it is irregular or continuously sloping without a shelf break.

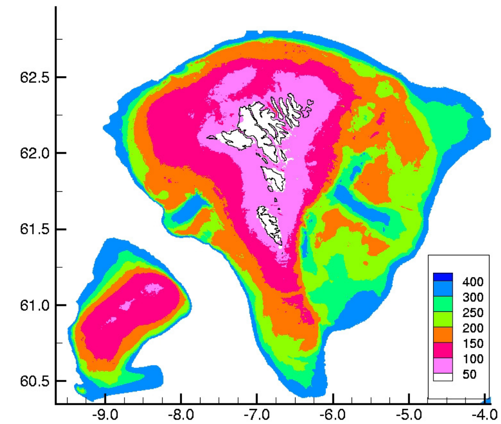

Figure 1. The Faroe Plateau and the Faroe Bank.

Because of strong tides, the on-shelf water is well mixed throughout the year, while the off-shelf water can be stratified in the summer season. In winter the cooling is on the other hand more efficient on the shelf (Fig. 2). This creates a temperature front, not only in the summer season, but also almost throughout the year, except for the period October/November. The temperature front is most pronounced in the spring before the onset of off-shelf stratification and least pronounced or non-existing in the autumn, when the stratification is broken down.

The water inside the front occupies a special role in the Faroese marine ecosystem (Gaard *et al*., 2002), and the exchanges of water and various properties across the front are also assumed to be very important from the biological point of view. Acquiring more detailed knowledge about the front is therefore a high priority and here we use sea surface temperature data measured by a research vessel logging system to map the front. From these observations we have analysed the seasonal temperature variation and related it to a heat balance model. The location and width of the front are investigated in order to establish possible relations between these characteristics and the Lunar fortnightly tidal cycle and topography. The existence and position of the front is also discussed in relation to different theories of how front locations depend on the tidal currents. Simpson and Hunter (1974) suggested that the front is at contours of H/U^3, where H is the bottom depth and U^3 is averaged over a tidal period. Soulsby (1983) and Stigebrandt (1988) on the other hand suggested, that the front is at contours of H/U. Also, is the possibility of a shelf-break-front discussed.

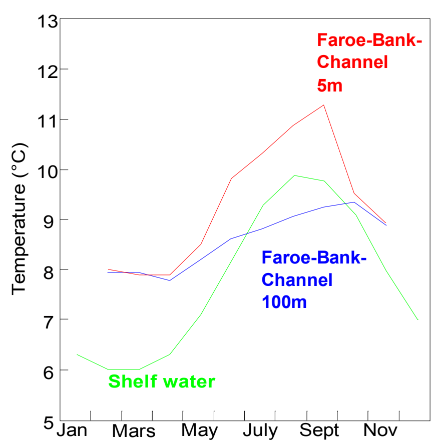

Figure 2. Monthly mean temperature (°C) on the shelf (green) and in the Faroe Bank Channel at 5 m depth (red) and 100 m depth (blue) representing off-shelf water. The temperature on the shelf is based on measurements at Mykineshólm 1914-69, while the temperatures in the Faroe-Bank-Channel are based on measurements from R/V Magnus Heinason 1982-97. Adapted from Hansen, 2000.

DATA MATERIAL AND METHODS

The temperature measurements consist of 92 crossings of the Faroe Shelf front by the R/V Magnus Heinason in the period February 1999 – November 2000. All months are represented, except for January and December. The R/V Magnus Heinason is equipped with a measuring system, where position (DGPS), bottom depth and sea surface temperature (SST) at approx. 3 m depth are measured continuously and saved every 10 seconds with the time of the measurement. From these data, tracks crossing the 50 and 200 m depth contours and/or tracks with continuously increasing (or decreasing) depth between 50 and 200 m have been selected.

Quality control and calibration

The measured data have been quality controlled by a standard procedure based upon data variation with time in relation to neighbouring data values (spikes). The editing has been done partly automatically (excluding extreme values) and partly manually using an interactive graphical software package developed by the Faroese Fisheries Laboratory (FFL), based upon MATLAB.

The SST data have been calibrated against CTD data. On cruises where CTD stations were operated, CTD stations showing a homogeneous surface layer, and where the SST at the same time showed a steady temperature, have been selected. For these stations, SST was plotted against CTD temperature from a shallow depth and this showed a linear relationship, y=ax+b. Figure 3 is an example of such a plot. For all the cruises the coefficient 'a' was constant within +/- 1%. The coefficient 'b' on the other hand was somewhat varying, but is assumed constant within each cruise. For cruises without CTD stations, the coefficient 'b' is interpolated linearly from the closest CTD cruises. The calibrated SST will typically have a relative accuracy of about 2%.

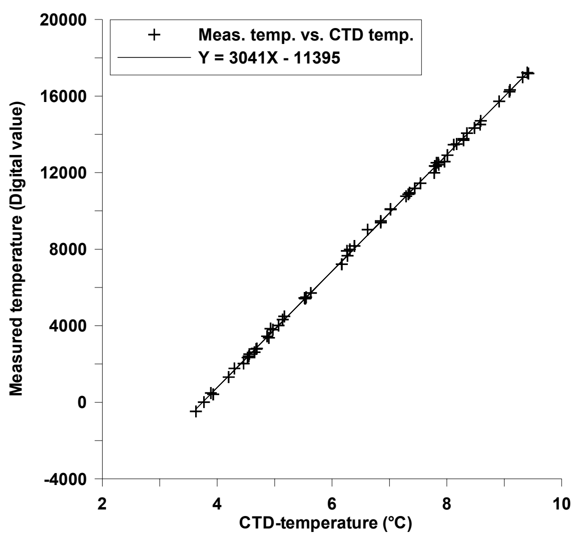

Figure 3. Calibration of measured SST (from approx. 3 m depth) vs. CTD surface temperature (from 3-5 m depth) on cruise 9932.

Exponential fit

For all tracks, the SST has been plotted against bottom depth. Many of these plots show a smooth or S- shaped step variation (Figures 4 and 5), with temperature increasing with depth. Therefore all plots have been fitted to two exponential functions:

$$F1(D) = A + B \times \exp[C(D - D0)];\; F2(D) = A + 2B - B \times \exp[-C(D - D0)] \quad (1)$$

A Fortran program has been written to make a "least square fit", finding the centre depth (D0) of the step and fitting depths shallower than D0 to function F1(D) and depths larger than D0 to the function F2(D) (Eq. 1). For some of the tracks, the program gave a good fit, but for others, the fit was poor because of e.g. irregularities or short tails in the temperature/depth plot. Many of the fittings have thus been adjusted manually. Figure 4 is an example of an exponential fit of the SST, showing the functions F1(D) and F2(D).

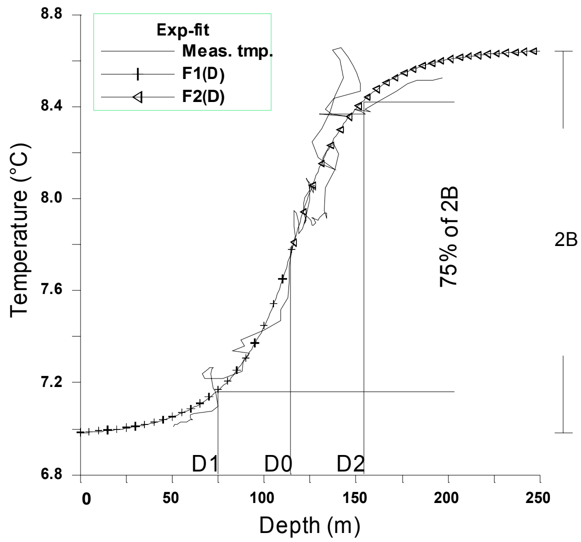

Figure 4. SST vs. bottom depth and exponential fit of the plot. D0 is centre depth of the front; D1 and D2 are inner and outer depth at the mid 75% temperature increase of the exponential fit (100%=2B).

Classification

For further analysis the data have been sorted by data quality and by geographic location. Regarding data quality the tracks are grouped into four minor groups, where each group has specific demands on the data quality, i.e. the straightness of the track, and the regularity of the temperature change vs. depth. The groups are listed in Table 1 with specification and number of tracks in each group. Figure 5 shows an example of a SST vs. bottom depth plot for each of the four groups.

Table 1. The table lists group identity, specification for each group and number of tracks in each group.

Group	Specification	No. of tracks in group
I	1. Track is a straight line 2. Depth is continuously increasing/decreasing 3. Temperature is continuously increasing/decreasing	15
II	1. Track is a straight line 2. SST vs. Bottom depth plot can have small irregularities 3. Fit of exp. function can be used to estimate mid-depth and width of the front.	27
III	1. Track can have small fluctuations 2. SST vs. Bottom depth plot can have irregularities 3. Fit of exp. function can be used to estimate mid-depth of front.	16
IV	1. Track can have fluctuations 2. SST vs. Bottom depth plot can have large irregularities 3. Can not be fitted with an exp. Function	34

The tracks have also been grouped into eight geographic groups according to track direction from the shelf area and the topography of the shelf. For example, north of the Faroes, the shelf is wide and slowly deepening and covers several track directions. Therefore, directions with only few tracks are grouped together with neighbouring directions, if the topography is similar. Figure 6 shows all the tracks covered in this report with lines and letters showing the different geographic groups.

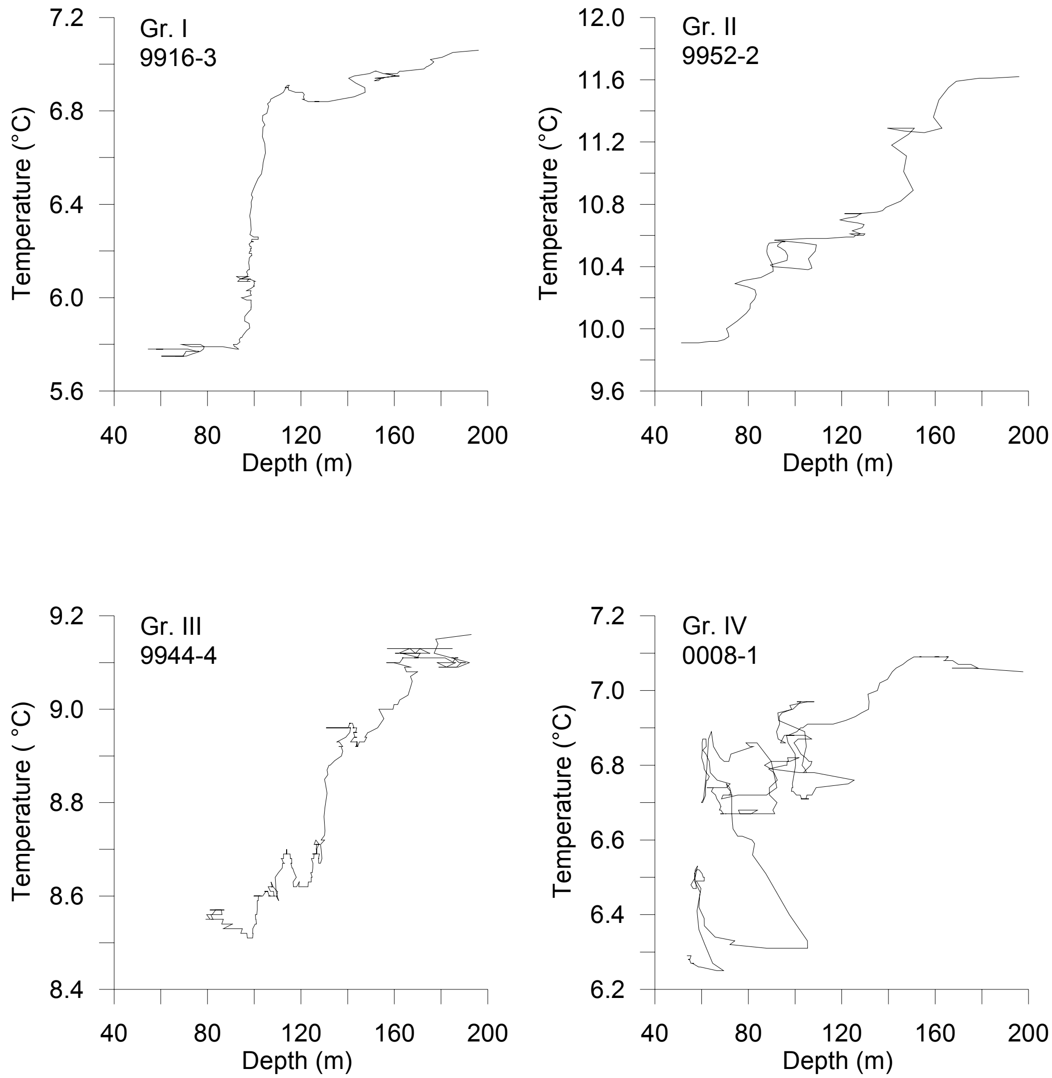

Figure 5. Examples of SST vs. Bottom-depth plot from group I, II, III and IV, respectively. The tracks are randomly chosen within each group.

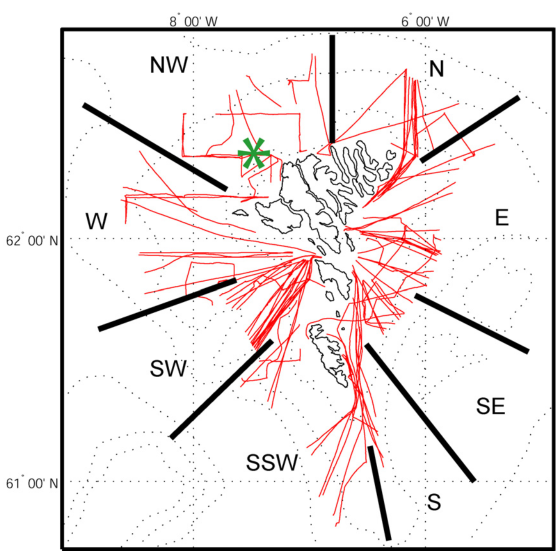

Figure 6. Track plot of 92 tracks on the Faroe Shelf. Thick lines are separation lines for direction groups. The letters are direction names. The green star in the NW direction is the position of Aanderaa Current Meter deployment 2985_010.
The contour lines in this Figure and Figure 11, 12 and 13 are from GEBCO 95.

RESULTS

Temperature change across the front

The on-shelf water temperature is almost always lower than the off-shelf water temperature. Only five of the 92 crossings of the front showed warmer water on the shelf. These five observations were from the months September, October and November and they all had a temperature difference lower than half a degree C. The data from all the 92 crossings show that the temperature difference between absolute maximum and absolute minimum along the track varies from -0.48 to 2.16 °C, where the minus sign indicates that the water is warmer on the shelf (Larsen *et al.*, 2001). In Figure 7, numbers of observations of temperature differences greater than 1.0 °C and lower than 0.5 °C, respectively are plotted against the month of observation. The figure shows, that temperature differences greater than 1.0 °C most often occur from March to June, while temperature differences less than 0.5 °C are most common from September to February. Unfortunately the months January and December are not represented in the data set.

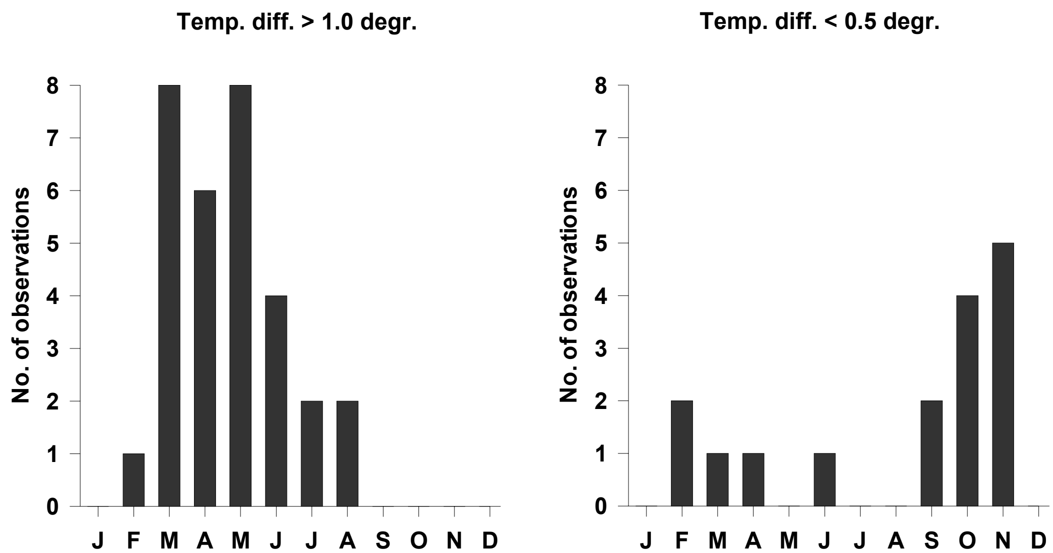

Figure 7. The left plot shows number of observations vs. month, where the cross frontal temperature difference exceeded 1.0 °C. Only crossings of type I, II and III in Table 1 are included. The right plot shows number of observations vs. month, where the temperature difference was less than 0.5 °C. Here most observations are of type IV, and only one, which did not have a straight track, was excluded.

From the exponential fit (Eq. 1), the B coefficient multiplied by two is an estimate for the temperature difference across the front (Figure 4). A plot of 2B against month should thus show the same pattern as in Figure 7. This is plotted in Figure 8 for all tracks in group I and II. As above, it is found that the largest differences occur from early spring to summer and are not found in the winter season, while small differences are most common from late summer and can occur until next spring.

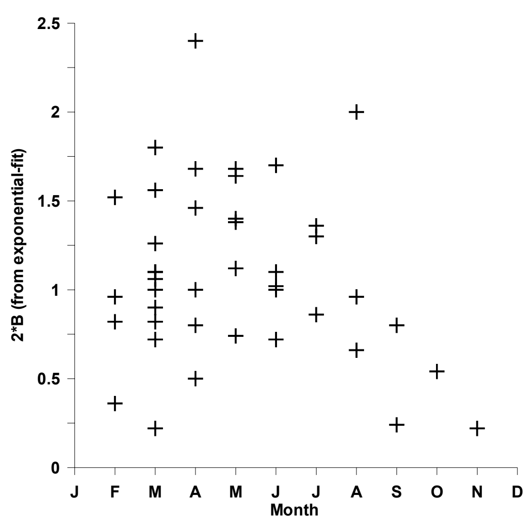

Figure 8. 2B coefficient from exponential fit (Eq. 1) vs. month of observation. All tracks (42) in group I and II are included.

Location and width of the front

For seven directions the mean D0 depth, which is the centre depth of the front estimated from the exponential fit, is calculated for all tracks in group I, II and III (direction S is excluded, because it has too few tracks in these groups). As an indication of the width of the front, the depths corresponding to the middle 75% of the exponential fit, shown as D1 and D2 in Figure 4, were found. For this estimation, only tracks in groups I and II are included, because in these groups, the temperature profile is estimated to be good enough to also fit the 'tails' of the exponential functions. Table 2 lists the mean of D0, D1 and D2 for each of the seven directions.

Table 2. The table lists for seven directions (Fig. 6) the calculated mean for depths D0, D1 and D2 and their respective standard error. For D0 all tracks in group I, II and III are used, while only tracks from group I and II are used for calculation of the mean of D1 and D2. Also listed are the difference between D1 and D2 and the number of tracks included in the calculations of D0, D1, and D2.

Direction	Mean D0 (m)	Std. Err. for D0	Mean D1 (m)	Std. Err for D1	Mean D2 (m)	Std. Err for D2	D2-D1	No. of tr. D0	No. of tr. D1, D2
E	105	5	47	12	149	12	102	13	10
SE	87	3	52	12	108	8	56	8	6
N	114	6	70	10	164	18	94	8	6
NW	104	4	90	1	113	1	23	6	2
SW	141	6	103	16	177	10	74	10	8
SSW	163	6	153	10	203	12	50	6	4
W	153	8	111	15	178	16	67	5	4

The values in Table 2 show, that the centre depth, D0, is much deeper for the three directions west, southwest and south southwest than for any other direction.

In Table 2 is also listed the vertical extent of the front as D2-D1, i.e. the depth range, which the front is covering. The smallest depth range is found in the direction northwest, which also is the widest and flattest area of the shelf. The largest depth ranges are found in the north and east directions, and these directions have the most continuously increasing bottom depth without large steps in the topography, that is covered by the tracks.

To investigate a possible frontal movement with the neap-spring cycle (Lunar fortnightly), normalised depth anomaly from 58 tracks from the groups I, II and III have been plotted in Figure 9 against the cube of the velocity averaged over the last seven days before the track event (including the day of the track event). Since the mean depth is varying for each direction, the depth is normalised according to its direction. The velocity is a prediction calculated from an Aanderaa Current Meter time series – deployment 2985_010 (Hansen & Larsen, 1999) at a position northwesterly on the Faroe Shelf (Fig. 6). The length of the time series is about 6½ months. The correlation coefficient for the values in Figure 9 was only 0.06, and thus not significant.

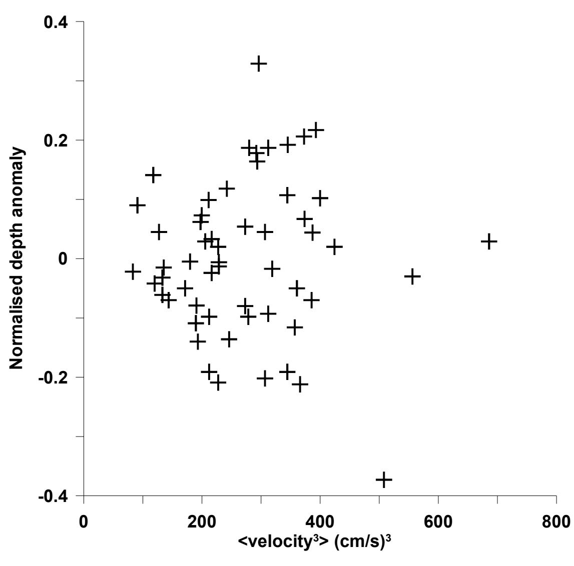

Figure 9. Normalised depth anomaly vs. the cube of predicted velocity averaged over seven days. The predicted velocity is first calculated every 12 minutes. These values are cubed. Then the average for the day of the track and six days before the track is calculated. For normalising the depth, the mean depth in each direction is calculated. The normalised depth anomaly is then the actual depth minus mean depth divided by the mean depth for the actual direction. All tracks (58) from group I, II and III are included.

The same procedure has been made on 42 tracks from the months March, April, May and June, when the temperature difference across the front is most pronounced. The depths have been renormalised to include these 42 tracks only, and are again normalised according to their direction. These results are plotted in Figure 10. The correlation coefficient for this plot is 0.09, so there is again no significant correlation.

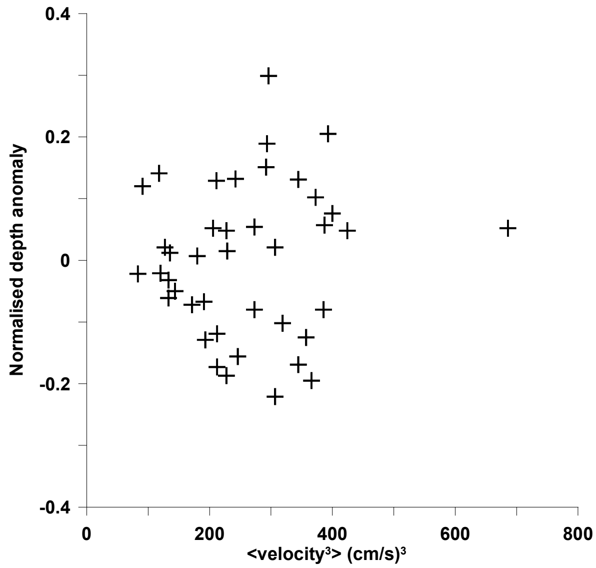

Figure 10. All tracks (42) from group I, II and III in the months March, April, May and June are included. For explanation of calculating the averaged velocity and normalised depth anomaly, see text for Figure 9.

FRONTAL THEORIES

We shall here briefly describe three possible frontal theories, and look at how they fit to the front on the Faroe Shelf. These are the H/U^3 and H/U, which have been much discussed in the last three decades in relation to tidal fronts and finally we shall look at the possibility of a shelf-break-front. In testing H/U^3 and H/U we have used velocity data from a tidal model by Simonsen (1999). We use the depth mean M2 amplitude averaged over a tidal period (Appendix A), since this is generally accepted in similar work (Simpson, 1998).

H/U^3

Simpson and Hunter (1974) established a frontal theory based on energetic considerations. They postulated, that if an amount of heat is added at the surface, this heat adds buoyancy to the surface water. To overcome this buoyancy and mix it through out the water column you need a certain amount of turbulent energy, in this case assumed supplied by the tide. The position of the front will then be, where the tidal energy is large enough to mix the added buoyancy at the surface through the whole water column. This theory is reported in many papers, and the final equation is set up in many forms. We here reproduce the equation given in a paper by Loder and Greenberg (1986):

$$\frac{H}{D_t} = \frac{2C_p \varepsilon_t}{g \alpha Q} \text{ where } D_t = \rho C_d U^3 = \rho C_d \left\langle \left(u^2 + v^2\right)^{3/2} \right\rangle \qquad (2)$$

H is the bottom depth at the location of the front, C_d is the bottom drag coefficient, ρ is the density of seawater, C_p is the specific heat of seawater, ε_t is tidal mixing efficiency, since only a fraction of the tidal energy is used to mix the water column, g is gravitational acceleration, α is the thermal expansion of seawater and Q is the heat flux.

Since the net heat flux at the Faroe Islands is positive only from May to August (Lindau, 2001), this theory can only predict the position of the front in these months. Adjusting Q to the local area to a value between 40 and 100 W/m^2 in the summer season (Lindau, 2001) and calculating D_t using the M2 velocity cubed (as described in Appendix A) from the tidal model (Simonsen, 1999) we find, that H/D_t (in SI-units) should be 510 and 204 for the two respec-

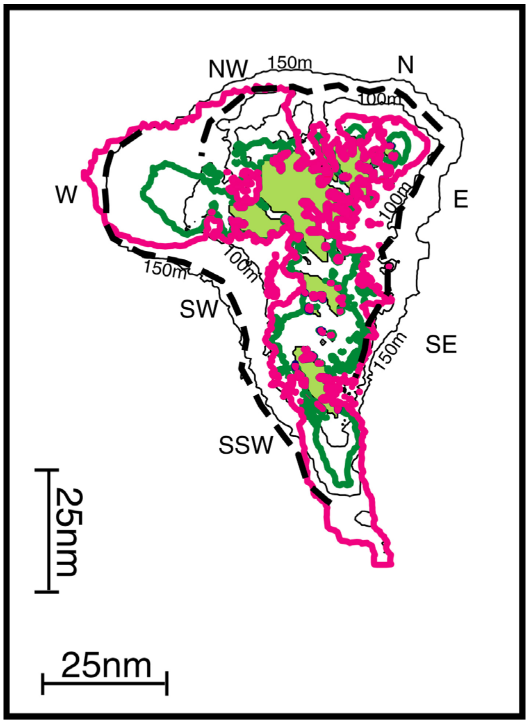

tive values of Q, or that log10 (H/D_t) should be 2.7 and 2.3, respectively. Figure 11 is a plot of log (H/D_t) at constant values 2.3 and 2.7.

Figure 11: Part of model domain (Simonsen, 1999) with 100 and 150 m bottom contours. Also plotted is the log (H/D_t) contours at 2.3 (green) and 2.7 (magenta), where H is the tidal model bottom topography and D_t is calculated using C_d=0.0026 and the M2 velocity cubed from the tidal model as described in Appendix A. The dashed black lines are the results from the SST measurements and show the mean location of the front grouped in directions (see Table 2).

It is seen in Figure 11, that the curve representing Q = 40 W/m^2 only in the northwest corner is similar to the measurements, while the remainder of that curve as well as the curve representing Q = 100 W/m^2 predicts the front to be at a shallower location.

H/U

Another theory on tidal fronts, but which is not seasonally dependent, is based on bottom and surface Ekman layers, where the bottom Ekman layer arises from tidal streams, while the surface Ekman layer arises from wind. Loder and Greenberg (1986) and Stigebrandt (1988) ignore the surface Ekman layer and use the bottom Ekman layer only and they find good agreement in the Irish Sea and The Gulf of Maine. The equation they use is:

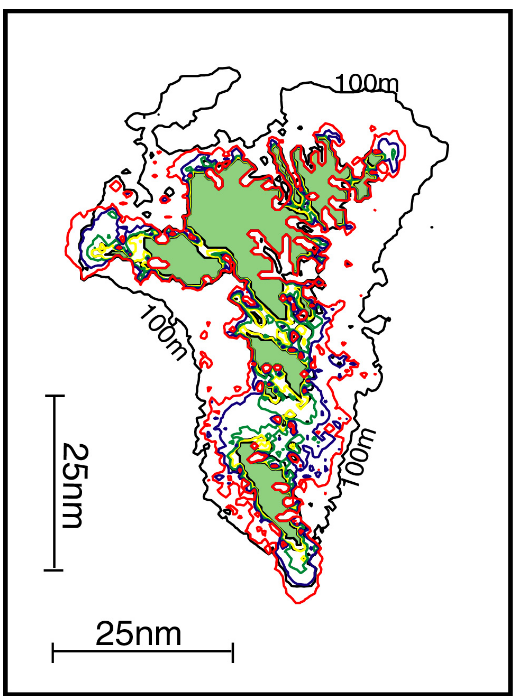

$$\frac{H}{U} = \frac{\lambda\sqrt{C_d}}{f} \qquad (3)$$

where λ = 0.2 and f is the local Coriolis parameter. Loder and Greenberg (1986) imply, that λ is usually in the range 0.1 to 0.4, and the result for four values in this range is plotted in Figure 12, where again the velocity is drawn from the tidal model (Appendix A).

It is seen (Fig. 12), that all the curves are within the 100 m bottom contour and do not fit the observations drawn as dashed lines in Figure 11.

Figure 12. Contours of H/U = $\lambda(C_d)^{1/2}/f$. C_d=0.0026, f=1.28e-4, λ=0.1(yellow), 0.2(green), 0.3(blue) and 0.4(red).

Soulsby (1983) includes the rotation of the tidal ellipses, where the bottom layer thickness then is given by

$$\delta_+ = \frac{C\sqrt{C_d}U}{\sigma + f} \quad \text{and} \quad \delta_- = \frac{C\sqrt{C_d}U}{\sigma - f} \qquad (4)$$

for the cyclonic and anti-cyclonic rotations, respectively. σ is the frequency of the tidal constituent M2 and C is a constant (Soulsby, 1983). Soulsby (1983) then combines these depths to a weighted mean boundary layer, which is

$$\delta = C\sqrt{C_d}\,\frac{U_{maj}\sigma - U_{\min} f}{\sigma^2 - f^2} \qquad (5)$$

where U_{maj} and U_{min} are the major and minor semi-axis in the tidal ellipses, respectively. In Figure 13 is H/δ = 1 plotted, where δ is calculated from Eq. 5 with C=0.075 (Soulsby, 1983) and the M2 tidal semi-axis from Simonsen (1999).

It is seen (Fig. 13), that the prediction of the frontal location of the H/U theory with inclusion of the rotation of the tidal ellipses fits fairly well to the observed location of the front except for the southwest and south southwest directions.

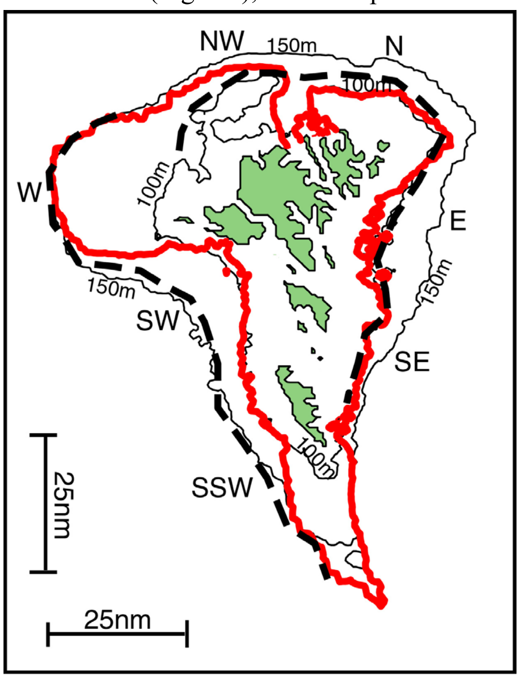

Figure 13. Contour of H/δ = 1, where δ is as defined in Eq. 5.

Shelf-break-front

A shelf-break-front is often observed at the break of flat shelves. It extends from the bottom at the break of the shelf to the surface, but can also extend only to mid depth, if the surface layer is stratified (Gibbs *et al.*, 2000). In the latter case it can of course not be observed with SST measurements.

The Faroe Shelf has only in some areas a well-defined shelf-break, where it is easy to define a shelf-break-front. Plots of temperature and depth vs. distance, from tracks normal to the depth contours only, show that the front is sometimes at the shelf-break or within 5 km of it. At other times it is around 10-20 km within the shelf-break, which in most areas is on the order of the width of the shelf.

DISCUSSION

The SST measurements show, that the front around the Faroe Shelf is a dynamical system. Some times the front is sharp and well defined, and other times it is more diffuse. In Figure 2 is seen, that the front is most pronounced in the early spring before the onset of off-shelf stratification and this is also confirmed in the SST measurements (Fig. 7). This temperature difference between the on-shelf water and the off-shelf water can in a simple manner be explained in terms of a heat budget. The net air-sea heat flux is negative for eight months of the year and only positive for the summer months May to August (Lindau, 2001). Because the shelf is shallow and well mixed, it is more effectively cooled when the net air-sea heat flux is negative and we could thus expect to find, that the temperature is continously increasing from shallow to deep water. Using the bottom topography from the tidal model (Simonsen, 1999) we have calculated the seasonal heat balance of the shelf and its surroundings (Appendix B). The result is plotted in Figure 14, where the extreme curves can be considered as representing the on-shelf water (red curve) and the off-shelf water (blue curve), when we do not take into account the off-shelf stratification. Comparing these two curves to the on-shelf (green) and off-shelf (blue – 100 m depth) curves in Figure 2, we find, that the calculated heat balance reproduces the seasonal temperature variation to a reasonable degree.

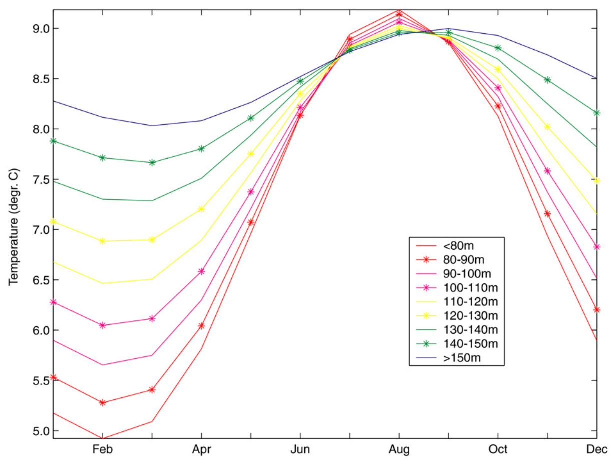

Figure 14. Heat balance through the year calculated for 9 assumed water columns (Appendix B).

In Figure 2 it may look like that the seasonal termocline off-shelf is well established, but measurements show, that this is only true for the month of July – in the other summer months, the seasonal termocline is only transient (Hansen, 2000). This fact might be one of the reasons for, that we find the H/U^3 theory insufficient (Fig. 11).

In considering the possiblitiy of a shelf-break-front we find, that the Faroe Shelf only in a few areas has a well-defined shelf break. Although the SST measurements alone are insufficient in investigating a shelf-break-front, this solution is discarded as a general explanation of the location of the front.

In testing the H/U theory we find, that a bottom Ekman layer, as used by Loder and Greenberg (1986) and Stigebrandt (1988), can not explain the location of the front (Fig. 12), but in a weighted mean boundary layer, as by Soulsby (1983), where the rotation of the tidal ellipses is added, we find a fairly good agreement with the observed location of the front (Fig. 13). Only the bottom depth at the front location in the southwest and south southwest are somewhat underestimated. One reason for this might be that the M2 velocity in the tidal model is slightly underestimated (Simonsen, 1999). Another reason might be, that the H/U theory, discussed here, is not the whole story. We have already mentioned, that the surface Ekman layer is ignored and this might not be a good assumption for the Faroese region, which is generally considered as windy (Cappelen and Laursen, 1998).

In the observations of the front we have found, that the front is at deeper locations in the directions west, southwest and south southwest (Table 2). Simpson (1998) points out, that in the H/U theory including the rotation of the ellipses not only the strength of the tide, but also the polarisation (i.e. minor/major) of the tidal ellipse controls the position of the front. As seen in Figure 15, the absolute polarisation increases towards the off-shelf water, especially west of the Faroes and in the southwest direction and thus fits the pattern of the observed mean depth of the front (Table 2).

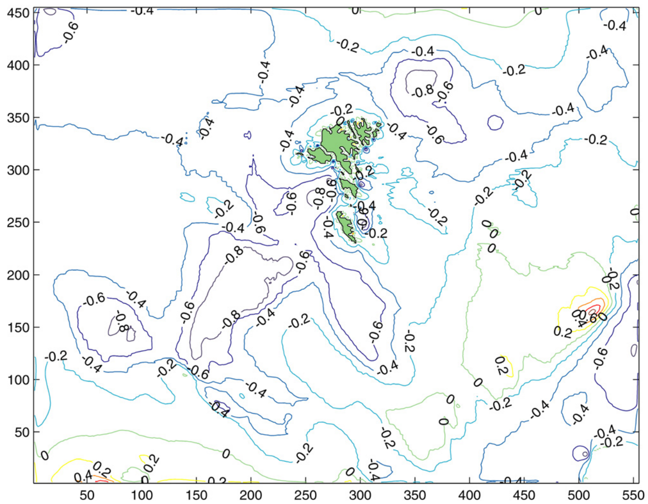

Figure 15.
Polarisation of the M2 tidal ellipse (P = U_{min}/U_{maj}) calculated from the tidal model (Simonsen, 1999). Negative polarisation refers to anti-cyclonic rotation.

But this asymmetry in frontal depth is in Figure 13, only predicted for the direction west. To explain this, we assume, that the front is at the location, where the surface mixed layer plus the bottom mixed layer equal the bottom depth, and that the surface mixed layer has a similar asymmetry with deeper depths in the southwesterly directions, since the most frequent wind direction in the area is from southwest (Cappelen and Laursen, 1998). Together with an adjustment of the constant C (Eq. 5), this could give a better fit to the observations, but this as well as other possibilities (e.g. intensification of other tidal constituents and tidal/residual advection of the front) are left for future investigations.

CONCLUSION

We have found, that the temperature difference across the Faroe Shelf front is most pronounced in the spring, and that this can be explained by a simple heat budget – the on-shelf water is more effectively cooled during winter than the off-shelf water, creating a large temperature difference between the water masses in the early spring.

The position of the front vs. bottom depth is discussed in relation to several theories and it is found, that the theory by Soulsby (1983) best fits the observed position of the front, as long as the surface mixed layer is ignored. The frontal bottom depth is found to be larger west of the islands than north and east of the islands. The reason for this is believed to arise from larger anticyclonic polarisation of the tidal ellipse and from frequent winds from the south-west direction.

APPENDIX A

The tidal model

The tidal model used in this analysis is from Simonsen (1999). The model describes the entire Faroe Plateau and the surroundings to the south and west. It has a grid size of 0.5x0.5 nautical miles and has 455 x 555 grids. It is a barotropic model, meaning that it only has one layer, and that the current is assumed to be the same through the whole water column. This is fairly realistic for the on-shelf water, but not for off-shelf waters (Larsen *et al.*, 2000). Figure 16 shows the model domain with bathymetry.

The output from the model is both elevation and current data and includes eight constituents: K1, K2, M2, N2, O1, P1, Q1 and S2. The current data is represented with the tidal ellipse parameters. In calculating the tidal current, we only use the parameters major and minor, since we only calculate the length of the velocity vector and not the direction. It can be noted, that the M2 semi axes are somewhat underestimated as a whole in the model.

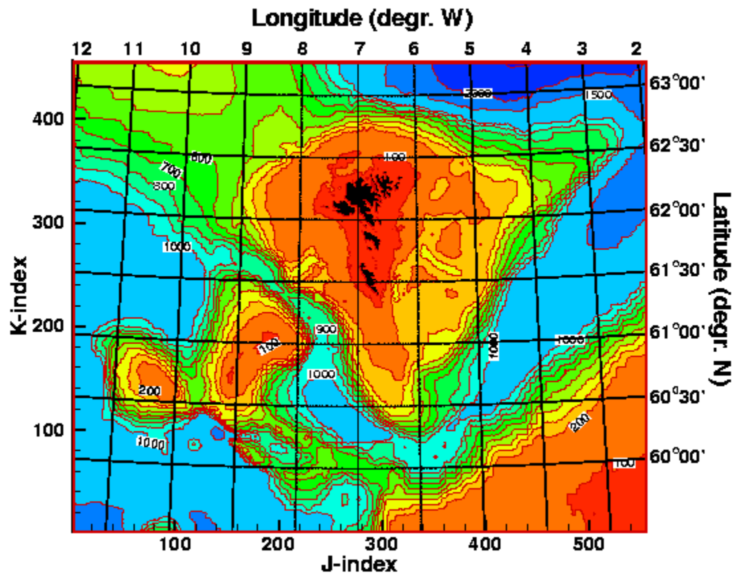

Figure 16. Model domain and bathymetry.

Data from the model

To calculate the mean M2 speed (U) and M2 speed cubed (U^3), the M2 major (A) and minor (B) semi-axes matrixes from the model are used, where each number in the matrix represents a grid point. Time averaged over a tidal period (T), the M2 speed becomes:

$$U = \left(\frac{1}{T} \int_0^T \left(A^2 \cos^2(\omega t) + B^2 \sin^2(\omega t) \right) dt \right)^{1/2} = \left(\frac{1}{2} \left(A^2 + B^2 \right) \right)^{1/2} \quad \text{where } \omega = \frac{2\pi}{T} \qquad (6)$$

while the M2 speed cubed becomes

$$U^3 = \frac{1}{T} \int_0^T \left(A^2 \cos^2(\omega t) + B^2 \sin^2(\omega t) \right)^{3/2} dt \qquad (7)$$

where the integration is done in a Matlab routine. These velocities are then used to calculate H/U^3 and H/U, where H is the topography matrix from the model.

APPENDIX B

Heat balance of the Faroe Shelf

We calculate the seasonal heat balance of the Faroe Shelf using a monthly mean net air-sea heat flux from Lindau (2001) and the bottom topography matrix from the tidal model (Appendix A). We assume, that the water column is steady in the sense, that the water inside the column is not advected, and to make the calculations simple, a heat gain or loss at the surface is immediately distributed throughout the column. Further, a heat flux is allowed through the sides of the water column to adjacent columns.

The topography matrix is divided into assumed curved blocks, where the inner and outer sides of each block follow two different bottom contours. The water mass inside the 80 m bottom contour is considered as the innermost water column with homogenous water. The adjacent water column is the water mass between the 80 and 90 m bottom contours, the next water column is between the 90 and 100 m bottom contour and so on extending to the 150 m bottom contour. The off-shelf water column is considered as homogenous from the 150 m bottom contour surrounding the Faroe Shelf extending horizontally to the border of the model domain, except for areas shallower than 500 m (e.g. the Scottish Shelf) and extending vertically from the surface to the bottom depth, though maximum down to 500 m, which is taken as the depth limit for convective mixing (Hansen & Østerhus, 2000).

The calculations start in October, where we consider, that all the water columns have equal temperature (Fig. 2). The calculations run for a year in time steps of one day, where the net air-sea heat flux is taken constant within each month. The heat diffusion through the sides of the water column to the adjacent columns is calculated at each time step, where the diffusion constant is equal for all columns. The temperature change at each time step of the i'th column is:

$$\Delta T_i = \frac{\Delta t}{C_p \rho V_i}\left[Q A_i^{surf} - k A_{i-1}^{side}(T_{i-1} - T_i) + k A_i^{side}(T_i - T_{i+1}) \right] \tag{8}$$

where Δt is the timestep, C_p is the specific heat of seawater, ρ is the density of seawater, V_i is the volume of the i'th water column, Q is the net air-sea heat flux, A_i^{surf} is the sea surface area of the i'th water column and A_i^{side} is the area of the side of the i'th water column, calculated as depth times the circumferrence $C = \sqrt{\pi A}$, assuming, that the circumference of the water column can be calculated as the circumference of a circle, were the area A of the circle is known. Finally T_i is the temperature of the i'th water column and k is a diffusion konstant. For the innermost water column (i=1) the area A_0 is zero, since it only has one adjacent column. For the off-shelf water column T_{i+1} is not defined. Instead a constant heat input is supplied to balance the net heat loss through the surface of all the columns. This heat input can be regarded as representing the heat input from the North Atlantic Current and is assumed constant.

The value of k was found by running the calculation several times for different values of k and then selecting the result, which best fit the temperature variation in Figure 2. The selected value of k is consistent with typical values for the turbulent diffusivity in open ocean.

The result of the calculation is shown in Figure 14, where the temperature at the end of each month is plotted for each water column.

REFERENCES

1. Cappelen, J. and Laursen, E. V. 1998. The Climate of the Faroe Islands - with Climatological Standard Normals, 1961-1990. Danish Meteorological Institute No. 98-14, 62 pp.

2. Gaard, E., Hansen, B., Olsen, B., and Reinert, J. 2002. Ecological Features and Recent Trends in the Physical Environment, Plankton, Fish Stocks, and Seabirds in the Faroe Shelf Ecosystem. Large Marine Ecosystems of the North Atlantic, 245-265.

3. Gibbs, M. T., Marchesiello, P., and Middleton, J. H. 2000. Observations and simulations of a transient shelfbreak front over the narrow shelf at Sydney, southeastern Australia. Continental Shelf Reasearch, 20, 763-784.

4. Hansen, B. and Larsen, K. M. H. 1999. Traditional Current Meter Observations in Faroese Offshore Waters. The Faroese Fisheries Laboratory. Technical Report No. 99-01, 193 pp.

5. Hansen, B. 2000. Havið. Føroya Skúlabókagrunnur. Torshavn, 232 pp (in Faroese).

6. Hansen, B. and Østerhus, S. 2000. North Atlantic-Nordic Seas exchanges. Progress in Oceanography, 45, 109-208.

7. Larsen, K. M. H., Hansen, B., Kristiansen, R., and Østerhus, S. 2000. Internal tides in the waters surrounding the Faroe Plateau. ICES Annual Science Conference CM2000/L:09, 13 pp.

8. Larsen, K. M. H., Hansen, B., and Smith, L. 2001. The Front on the Faroe Shelf based on data logged by R/V Magnus Heinason 1999 - 2000. The Faroese Fisheries Laboratory. Technical Report No. 01-03, 13 pp.

9. Lindau, R. 2001. Climate Atlas of the Atlantic Ocean. Springer-Verlag. Berlin, 514 pp.

10. Loder, J. W. and Greenberg, D. A. 1986. Predicted positions of tidal fronts in the Gulf of Main region. Continental Shelf Research, 6, 397-414.

11. Simonsen, K. 1999. Tides and tidal simulation in the area around the Faroe Islands. Nansen Environmental and Remote Sensing Center. Technical Report No. 166, 104 pp.

12. Simpson, J. H. and Hunter, J. R. 1974. Fronts in the Irish Sea. Nature, 250, 404-406.

13. Simpson, J. H. 1998. Tidal Processes in Shelf Seas. *In* The Sea. The Global Coastal Ocean. Processes and Methods. *Edited by* K.H.Brink and A.R.Robinson. John Wiley & Sons, Inc., 113-150.

14. Soulsby, R. L. 1983. The Bottom Boundary Layer of Shelf Seas. *In* Physical Oceanography of Coastal and Shelf Seas. *Edited by* B.Johns. Elsevier Science, 189-266.

15. Stigebrandt, A. 1988. A note on the locus of a shelf front. Tellus, 40A, 439-442.